A Study on the Biocompatibility of Surface-Modified Au/Ag Alloyed Nanobox Particles in Zebrafish in Terms of Mortality Rate, Hatch Rate and Imaging of Particle Distribution Behavior

Kanghui Li[1], Xinyuan Zhao[2], Yixing Zhai[2], Guangdi Chen[2], El-Hang Lee[1], and Sailing He[1, *]

Abstract—We report for the first time a study on the biocompatibility of the poly(ethylene glycol)-thiol (PEG)-coated Au/Ag alloyed nanobox (PC-ANB) particles in zebrafish. We measured the mortality rate and the hatch rate of the zebrafish embryos injected with the PC-ANB particles and observed the distribution of the PC-ANB particles in the zebrafish embryos at different stages of growth development. The results show that the PC-ANB particles have negligible toxicity to the zebrafish embryos even at extrahigh concentration ($1.2\,\mathrm{mg\,ml^{-1}}$), while uncoated Ag nanoparticles, used in the form of nanospheres or nanoplates, were found to cause embryo deformation or even death. Additionally, we have investigated the distribution of the PC-ANB particles within the zebrafish in the interest of studying their behavior in the zebrafish using imaging. For this, we used the three-photon luminescence imaging technique and it has been found that the PC-ANB particles mainly assemble in the backside muscle tissues of the zebrafish, suggesting that the PC-ANB particles are mostly metabolized out after about 96 hours of growth development.

1. INTRODUCTION

Metal nanoparticles have been given much attention in recent years in the study of nanoscience and nanotechnology due to their unique properties. They are used in the study of diverse areas such as photocatalysis [1], biosensing [2] and bioimaging [3] and exhibit many useful advantages. Compared with other nanoprobes such as organic fluorophores and quantum dots, metal nanoparticles are not easily susceptible to photobleaching or blinking, which is particularly important in the study of optical imaging of living organisms. Also, their distinctive localized surface plasmon resonance (LSPR) properties make metal nanoparticles promising for optical applications such as solar cells [4] or surface enhanced Raman scattering (SERS) studies [5]. Among various kinds of metal nanoparticles, Au/Ag alloyed nanobox (ANB) particles have received special attention as they can be synthesized fast in a relatively straightforward manner, and can provide widely tunable LSPR wavelength range and convenience in surface modification [6–8]. Despite the distinct utility of the ANB particles, however, the biocompatibility or the toxicity of these particles on the living organisms has not been reported to the best of our knowledge, although the toxicity of many other kinds of metal nanoparticles such as gold or silver nanoparticles has been studied [9–12]. It has been reported that when the ANB particles are used for *in vivo* applications, they are usually surface-coated with poly(ethylene glycol)-thiol (PEG) in

order to maintain their dispersity [8, 13]. It is therefore critically important to investigate the safety of these particles in their use for *in vivo* studies of living organisms.

Zebrafish is commonly used in studying the effect of the toxicity of nanoparticles due to several distinctly useful characteristics [14–17]. Firstly, zebrafish embryos grow fast. It normally takes only less than one week to develop major organ systems, thereby allowing a significant time-saving. Secondly, since the size of the zebrafish is small, it requires only a small sample volume for the study. Thirdly, due to its optical clarity in the visible range, it makes it possible to conduct a real-time noninvasive observation conveniently. The zebrafish is also useful because its fecundity is much higher than other vertebrate model systems such as mice or monkeys. We, therefore, have adopted the zebrafish in our study to test the toxicity of the PC-ANB particles on them.

Nonlinear optical bioimaging method has attracted much increased attention in the past decade because it has many distinct advantages over the commonly used linear optical bioimaging methods [18, 19]. Firstly, since the excitation wavelength is normally set in the near infrared (NIR) region to avoid the generation of auto-fluorescence, the signal to noise ratio can be significantly improved. Secondly, the photothermal effect of metal nanoparticles can be greatly reduced because the excitation wavelength is set far away from the LSPR wavelength of the metal nanoparticles. Thirdly, long-wavelength photons cause less photodamage on the biosamples due to their low energy. Considering both the absorption and scattering of the NIR light in the living organism, the spectral window ranging from 1600 nm to 1800 nm is believed to be the most suitable excitation wavelength for deep-tissue nonlinear optical bioimaging [20]. We, therefore, have adopted a 1550 nm femtosecond (fs) laser as the excitation source. Among various nonlinear optical signals emitted from the ANB particles under the long-wavelength fs laser excitation, the three-photon luminescence (3PL) is selectively used as the imaging signal because the tissues of the zebrafish organisms have weak 3PL signal under the long-wavelength fs excitation, thus leading to a high signal-to-noise (SNR) ratio imaging of the PC-ANB particles [13].

Experimentally, the PC-ANB particles, synthesized in our laboratory, were micro-injected into the zebrafish embryos for various investigations described below. To confirm the validity of our testing method, the effects of the uncoated Ag nanospheres and the Ag nanoplates injected to the zebrafish were also examined as a reference. It is concluded that the PC-ANB particles have little toxicity on the zebra fish embryos even at their extra-high concentration, while uncoated Ag nanoparticles were found to cause a severe mortality or deformation in the zebrafish.

In addition, in order to investigate the behavior of the PC-ANB particles within the body of the zebrafish, the distribution of the PC-ANB particles in the zebrafish at different stages of growth has been studied using the three-photon luminescence (3PL) of the PC-ANB under the excitation of 1550 nm fs laser. The use of 3PL signals from the PC-ANB particles provided a high signal-to-noise ratio (SNR) with respect to those from the zebrafish because the 3PL signals from the zebrafish tissues is relatively weak compared to those from the PC-ANB particles. The 3PL imaging results show that the PC-ANB particles mainly assembled in the backside muscle tissue of the zebrafish, suggesting that they are metabolized out after about 4 days of metabolism.

2. METHODS AND MATERIALS

2.1. Synthesis of PC-ANB Particles

The metal nanoparticles used in this study were synthesized according to the method reported by Aherne et al. [6–8]. First, the Ag nanospheres were produced by adding 0.25 ml of $500 \, \text{mg} \, \text{L}^{-1}$ poly(sodium styrenesulphonate) (PSSS) into 5 ml of 2.5 mM trisodium citrate, followed by an addition of freshly prepared 0.3 ml of 10 mM $NaBH_4$. Then a syringe pump was used to add 5 ml of 0.5 mM $AgNO_3$ at a rate of $2 \, \text{ml} \, \text{min}^{-1}$ to the solution under vigorous stirring. Ten minutes later, when the solution turned yellow, the preparation of the Ag nanospheres was completed.

The Ag nanoplates were then produced by using the Ag nanospheres as seeds. Six ml of 0.5 mM $AgNO_3$ was added to the solution mixed of 10 ml DI water, 200 μm of 10 mM ascorbic acid and 5 ml of as-prepared nanospheres at a rate of $2 \, \text{ml} \, \text{min}^{-1}$ under vigorous stirring. The reaction proceeded so fast that the Ag nanoplates were formed almost immediately after the addition of $AgNO_3$.
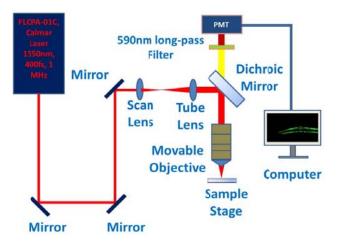
Figure 1. The optical set-up of 3PL imaging microscope.

The PC-ANB particles were finally prepared by using the Ag nanoplates as templates. First, a solution of 30 ml of 0.5 mM $HAuCl_4$ was added to the solution combining 3 ml of 10 mM ascorbic acid and 20 ml of as-prepared Ag nanoplates at a rate of $2\,\mathrm{ml\,min^{-1}}$ under vigorous stirring. The formation of the ANB particles was completed almost immediately after the addition of $HAuCl_4$.

Then, finally, they were surface-coated with PEG molecules by adding 30 mg poly(ethylene glycol)-thiol into the 50 ml as-prepared ANB solution followed by 5-minute vigorous stirring and undisturbed settling for 3 hours.

2.2. Characterization

First, the transmission electron microscopy (TEM) images of the metal nanoparticles were obtained by using JEOL JEM-1200EX microscope operating at 80 kV. The absorption spectra of the nanoparticles were obtained using Shimadzu 3600 UV-vis scanning spectrophotometer.

The 3PL imaging system used in our study consists of a 1550 nm fs laser source (FLCPA-01C, Calmar Laser, 1 MHz, 400 fs), an upright confocal microscope (Olympus BX61W1-FV1000) and an external photo-multiplier tube (PMT) whose response spectral region was 400 nm~900 nm. Figure 1 shows the schematic diagram of our optical set-up of 3PL imaging microscope. The output of the fs laser was directed into a scanning microscope as the excitation light, and the nonlinear optical signals were collected by the same objective (NA = 1.00, 20×, OLYMPUS). A 590 nm long-pass filter was inserted into the optical path to pick out the 3PL signals.

2.3. Zebrafish Lines and Maintenance

A zebrafish (Danio rerio) wild type AB stain was raised and maintained in the standard Zebrafish Unit (produced by Aisheng Zebrafish Facility Manufacturer Company, Beijing, China) at Zhejiang University under a constant 14 hour on/10 hour off light cycle at 28°C.

2.4. Embryos and Microinjection

The zebrafish embryos were collected at their one-cell stage and were transferred into an injection tray containing the system water. The uncoated Ag nanospheres (0.25 mM), Ag nanoplates (0.18 mM) and PC-ANB particles $(1.2\,\mathrm{mg\,ml^{-1}})$ were then injected into the yolks of embryos respectively. Each embryo was injected with approximately one nanolitre of the Ag nanospheres, Ag nanoplates or the PC-ANB particles. For the purpose of negative control, the embryos injected with one nanolitre of phosphate-buffered saline (PBS) were set aside as the control group.
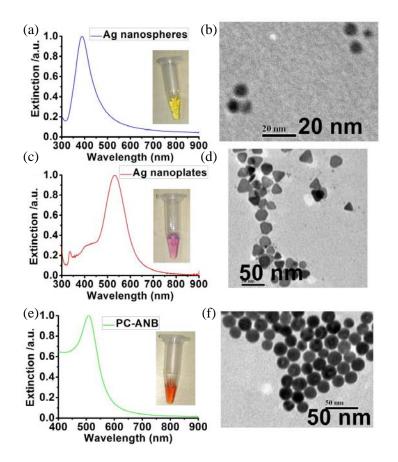
Figure 2. (a), (c), (e) Are the extinction spectra of Ag nanospheres, Ag nanoplates and PC-ANB, and the insets are the pictures of their corresponding solution, respectively. (b), (d), (f) Are the corresponding TEM images of the Ag nanospherers, Ag nanoplates and PC-ANB. The scale bars are 20 nm, 50 nm, 50 nm, respectively.

3. RESULTS AND DISCUSSION

3.1. Characterization of Metal Nanoparticles

Figure 2 shows the extinction spectra of the Ag nanospheres, Ag nanoplates and PC-ANB particles and their corresponding TEM images, respectively. The Ag nanospheres solution is yellow in color and its LSPR wavelength peak is at 390 nm. Its corresponding TEM image shows that the particle sizes were mainly below 10 nm. In the case of the Ag nanoplates, which were grown from the Ag nanospherers, their LSPR wavelength is red-shifted to 530 nm and their side lengths were about 20 nm on average. Lastly, the PC-ANB particles show voids in their interior. We speculate that the voids result from the redox reaction that took place during the synthesis process.

3.2. Study on the Effect of the PC-ANB Particles on the Zebrafish

In this study, the effects of the PC-ANB particles on the zebrafish were studied at several stages of the embryo development. First, the zebrafish embryos were exposed to the PC-ANB particles, Ag nanospheres and Ag nanoplates, respectively, in their one cell stage by microinjection. As shown in Figure 3, the toxic effect of the metal nanoparticles was examined by observing the mortality and hatch rates among the zebrafish embryos. Compared with the control group, the exposure of the embryos to the Ag nanospheres or Ag nanoplates significantly increased the mortality of the embryos at both the 24 hours post fertilization (24 hpf) stage and the 48 hours post fertilization (48 hpf) stage. However, the embryos injected with the PC-ANB particles showed no significant effect on the survival of the embryos

(Figure 3(a)). We next evaluated the effects of the PC-ANB particles on the hatch rate of the zebrafish embryos. Compared with the control group, a significant decrease ($P < 0.05$) in the cumulative hatching rate was observed at the 48 or 60 hpf stages for the Ag nanospheres or Ag nanoplates exposure group although the significant difference disappeared at the 72 hpf stage. However, the PC-ANB particles
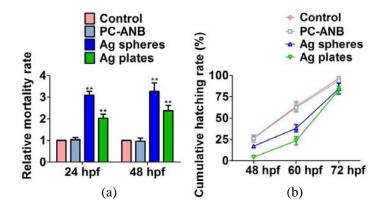

Figure 3. (a) Relative mortality rate of the zebrafish embryo exposed to the Ag nanospheres, Ag nanoplates or PC-ANB particles at 24 hpf and 48 hpf. (b) Cumulative hatch rate (%) of zebrafish embryo exposed to the Ag nanospheres, Ag nanoplates or PC-ANB particles at 48, 60 and 72 hpf. Asterisks ($*$) or ($**$) indicate the statistically significant differences as compared with the control group ($p < 0.05$) or ($p < 0.01$), respectively.
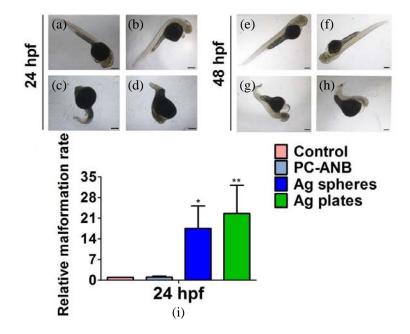

Figure 4. Morphological development of the normal (Control and PC-ANB) and malformed embryos in the Ag nanospheres or Ag nanoplates exposure groups. The representative images of the zebrafish embryos in the (a) control, (b) PC-ANB, (c) Ag nanospheres, or (d) Ag nanoplates exposure group at the 24 hpf stage, or in the (e) control, (f) PC-ANB, (g) Ag nanospheres, or (h) Ag nanoplates exposure groups at the 48 hpf stage. (i) Showing the relative malformation rate of the PC-ANB, Ag nanospheres, Ag nanoplates exposure groups at the 24 hpf stage. Asterisks ($*$) or ($**$) indicate the statistically significant differences as compared with the control group ($p < 0.05$) or ($p < 0.01$), respectively. The scale bars are 100 μm.

exposure did not show much change in the hatch rate of the embryos.

Figure 4 shows the biocompatibility of the metal nanoparticles as observed by the morphological development. At the 24 hpf stage, the control (Figure 4(a)) group and the embryos treated with the PC-ANB particles (Figure 4(b)) exhibited a normal development of the eyes, tails, or brain, whereas the embryos treated with the Ag nanospheres (Figure 4(c)) or Ag nanoplates (Figure 4(d)) exhibited shorter body length, spinal column, and the curving of the tail. And at the 48 hpf stage, we find more edema in pericardial sac in the Ag nanospheres (Figure 4(g)) and Ag nanoplates (Figure 4(h)) exposure groups. These results suggest lower toxicity and better biocompatibility of the PC-ANB particles compared with the uncoated Ag nanoparticles.

3.3. Distribution of the PC-ANB Particles within the Zebrafish at Different Growth Development Stages

The image of the zebrafish without any injected nanoparticles was first examined using the scanning microscope system as shown in Figure 1. To eliminate the 3PL signals of the zebrafish tissues, the parameters of an external photo-multiplier tube (PMT) were tuned gradually over a wide range. It turned out that when the integration time was set for 5 seconds and the gain at 65, no 3PL signal from the zebrafish tissues was observed, as shown in Figure 5.
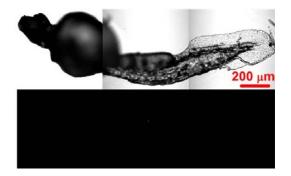

Figure 5. The transmission image and the 3PL image of the zebrafish embryo without any nanoparticles injected.
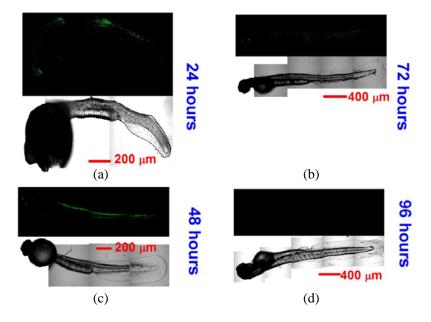

Figure 6. Distribution of PC-ANB in zebrafish at different development stages. (a)–(d) are 24 hours, 48 hours, 72 hours and 96 hours respectively.

Then the zebrafish embryos injected with the PC-ANB particles at different development stages were imaged under the same parameter settings. The thickness of zebrafish after 24∼96 hours' development is about 600∼700 µm, so we tuned the depth of focus to find the strongest 3PL signals when we imaged the zebrafish, and the pictures showed here were recorded when the depth of focus was around 200∼250 µm. Figure 6 shows the green-colored 3PL signals of the PC-ANB particles injected in the zebrafish and their corresponding transmission images. Figures 6(a)–(d) show the distribution of the PC-ANB particles in the zebrafish developed for 24 hours, 48 hours, 72 hours and 96 hours, respectively. As can be seen, the PC-ANB particles were found to be mainly distributed in the backside muscle tissues of the zebrafish, and the intensity of the green-colored 3PL signals were decreased with the development of the zebrafish. This result indicates that the amount of the PC-ANB particles in the zebrafish was gradually reduced due to the metabolism. Figure 6(d) finally shows that the PC-ANB particles were almost completely metabolized out of the zebrafish after 96 hours of growth development.

4. CONCLUSION

In conclusion, we have investigated for the first time the toxicity effect of the PC-ANB particles on the zebrafish embryos by observing the mortality rate and hatch rate of the zebrafish embryos injected with the PC-ANB particles. It is concluded that the PC-ANB particles have negligible toxicity on the zebrafish embryos even at an extrahigh concentration ($1.2\,\mathrm{mg\,ml^{-1}}$), while other kinds of Ag nanoparticles have highly negative influence on the zebrafish embryos. In addition, the study on the distribution of the PC-ANB particles in the zebrafish, examined at different developing stages utilizing the 3PL imaging of the PC-ANB particles, show that the PC-ANB particles mainly assemble in the backside muscle tissues of the zebrafish, suggesting that they were metabolized out almost completely after about 96 hours of growth development. This study suggests that the PC-ANB particles have a high biocompatibility level and that they can be effectively and widely applied in the study of nonlinear optical bioimaging of living organisms.

REFERENCES

1. Hou, W. and S. B. Cronin, "A review of surface plasmon resonance-enhanced photocatalysis," *Advanced Functional Materials*, Vol. 23, No. 13, 1612–1619, 2013.
2. Anker, J. N., et al., "Biosensing with plasmonic nanosensors," *Nature Materials*, Vol. 7, No. 6, 442–453, 2008.
3. Qian, J., et al., "Fluorescence-surface enhanced Raman scattering co-functionalized gold nanorods as near-infrared probes for purely optical in vivo imaging," *Biomaterials*, Vol. 32, No. 6, 1601–1610, 2011.
4. Till, J. H., et al., "Direct electrical evidence of plasmonic near-field enhancement in small molecule organic solar cells," *The Journal of Physical Chemistry C*, Vol. 118, No. 28, 15128–15135, 2014.
5. Zhang, Y., et al., "Multifunctional gold nanorods with ultrahigh stability and tunability for in vivo fluorescence imaging," *Angewandte Chemie International Edition*, Vol. 52, No. 4, 1148–1151, 2013.
6. Aherne, D., et al., "Optical properties and growth aspects of silver nanoprisms produced by a highly reproducible and rapid synthesis at room temperature," *Advanced Functional Materials*, Vol. 18, No. 14, 2005–2016, 2008.
7. Aherne, D., et al., "From Ag nanoprisms to triangular AuAg nanoboxes," *Advanced Functional Materials*, Vol. 20, No. 8, 1329–1338, 2010.

8. Liu, X. W., J. Lin, T. F. Jiang, Z. F. Zhu, Q. Q. Zhan, J. Qian, and S. He, "Surface plasmon properties of hollow AuAg alloyed triangular nanoboxes and its applications in SERS imaging and potential drug delivery," *Progress In Electromagnetics Research*, Vol. 128, 35–53, 2012.

9. Bar-Ilan, O., et al., "Toxicity assessments of Au and Ag nanoparticles in zebrafish embryos," *SMALL*, Vol. 5, No. 16, 1897–1910, 2009.

10. Lee, K. J., et al., "In vivo imaging of transport and biocompatibility of single silver nanoparticles in early development of zebrafish embryos," *ACS Nano*, Vol. 1, No. 2, 133–143, 2007.

11. Wang, Y. L., et al., "Biocompatibility and biodistribution of surface-enhanced raman scattering nanoprobes in zebrafish embryos: In vivo and multiplex imaging," *ACS Nano*, Vol. 4, No. 7, 4039–4053, 2010.

12. Asharani, P. V., et al., "Comparison of the toxicity of silver, gold and platinum nanoparticles in developing zebrafish embryos," *Nanotoxicology*, Vol. 5, No. 1, 43–54, 2011.

13. Li, K. H., et al., "Nonlinear optical properties of Au/Ag alloyed nanoboxes and their applications in both in vitro and in vivo bioimaging under long-wavelength femtosecond laser excitation," *RSC Advances*, Vol. 5, No. 4, 2851–2856, 2015.

14. George, S., et al., "Surface defects on plate-shaped silver nanoparticles contribute to its hazard potential in a fish gill cell line and zebrafish embryos," *ACS Nano*, Vol. 6, No. 5, 3745–3759, 2012.

15. Pan, Y., et al., "High-sensitivity real-time analysis of nanoparticle toxicity in green fluorescent protein-expressing zebrafish," *SMALL*, Vol. 9, No. 6, 863–869, 2013.

16. Fenaroli, F., et al., "Nanoparticles as drug delivery system against tuberculosis in zebrafish embryos: Direct visualization and treatment," *ACS Nano*, Vol. 8, No. 7, 7014–7026, 2014.

17. Kimmel, C. B., et al., "Stages of embryonic development of the zebrafish," *Developmental Dynamics*, Vol. 203, No. 3, 253–310, 1995.

18. Tong, L. and J. X. Chen, "Label-free imaging through nonlinear optical signals," *Materials Today*, Vol. 14, No. 6, 264–273, 2011.

19. Tong, L., et al., "Bright three-photon luminescence from gold/silver alloyed nanostructures for bioimaging with negligible photothermal toxicity," *Angewandte Chemie International Edition*, Vol. 49, No. 20, 3485–3488, 2010.

20. Horton, N. G., et al., "In vivo three-photon microscopy of subcortical structures within an intact mouse brain," *Nature Photonics*, Vol. 7, No. 3, 205–209, 2013.